

# Assessment of different bariatric surgeries in the treatment of obesity and insulin resistance in mice\*

**Mini-Abstract:** We developed mouse bariatric surgery models. Sleeve gastrectomy and mRYGB represent reliable restrictive and GI bypass mouse bariatric surgery models, respectively. Both restrictive and GI bypass procedures positively affect obesity and insulin resistance in the short term; however, the GI bypass shows better results than the restrictive procedure in the long term.

Deng Ping Yin, MD, PhD<sup>1,3</sup>; Qiang Gao, PhD<sup>1</sup>; Lian Li Ma<sup>1</sup>; Wenwei Yan, PhD<sup>1</sup>; Phillip E. Williams<sup>1</sup>; Owen P. McGuinness, PhD<sup>2</sup>; David H. Wasserman, PhD<sup>2</sup> and Najj N. Abumrad, MD<sup>1</sup>

1. Department of Surgery, Vanderbilt University Medical Center, Nashville, TN 37232
2. Mouse Metabolic Phenotyping Center, Vanderbilt University Medical Center, Nashville, TN 37232
3. Corresponding author: Deng Ping Yin, MD, PhD, Department of Surgery, Vanderbilt University Medical Center, e-mail address: [dengping.yin@vanderbilt.edu](mailto:dengping.yin@vanderbilt.edu)

\*This study was supported by NIH grant R01 DK050277 and DK059637 to D.W., JDRF grant 1-2008-159 to D.Y. and NIH grant R01 DK070860 to N.A.

Running head: Mouse bariatric surgery models

## Abstract

*Objective:* To assess the effects of different bariatric surgical procedures on the treatment of obesity and insulin resistance in high fat diet-induced obese (DIO) mice.

*Background:* Bariatric surgery is currently considered the most effective treatment for morbid obesity and its comorbidities; however, a systematic study of their mechanisms is still lacking.

*Methods:* We developed bariatric surgery models, including gastric banding, sleeve gastrectomy, Roux-en-Y gastric bypass (RYGB), modified RYGB (mRYGB) and biliopancreatic diversion (BPD), in DIO mice. Body weight, body fat and lean mass, liver steatosis, glucose tolerance and pancreatic beta cell function were examined.

*Results:* All bariatric surgeries resulted in significant weight loss, reduced body fat and improved glucose tolerance in the short term (4 weeks), compared to mice with sham surgery. Of the bariatric surgery models, sleeve gastrectomy and mRYGB had higher success rates and lower mortality and represent reliable restrictive and gastrointestinal (GI) bypass mouse bariatric surgery models, respectively. In the long term, the GI bypass procedure produced more profound weight loss, significant improvement of glucose tolerance and liver steatosis than the restrictive procedure. DIO mice had increased insulin promoter activity, suggesting over-activation of pancreatic beta cells, which was regulated by the mRYGB procedure. Compared to the restrictive procedure, the GI bypass showed more severe symptoms of malnutrition following bariatric surgery.

*Discussions:* Both restrictive and GI bypass procedures provide positive effects on weight loss, fat composition, liver steatosis and glucose tolerance; however, in the long

term, the GI bypass shows better results than restrictive procedures.

## Introduction

Obesity is associated with an increased risk of developing type 2 diabetes mellitus (T2DM) and cardiovascular disease. It has been described as the greatest current threat to human health and represents a major public health crisis<sup>1-3</sup>. Bariatric surgery is currently considered the most effective treatment for obesity and its comorbidities<sup>2,4</sup>. Beneficial effects of bariatric surgery include weight loss, reduced insulin resistance, and decreased risk factors for cardiovascular disease<sup>2</sup>. Based on the nutrient pass patterns, bariatric surgery is divided into two classes: restrictive procedures (e.g. gastric banding and sleeve gastrectomy) and gastrointestinal (GI) bypass procedures (e.g. Roux-en-Y gastric bypass, RYGB, and biliopancreatic diversion, BPD). Gastric banding is a purely restrictive procedure, and other surgeries, including RYGB and BPD, however, produce restrictive diet intake as well as malabsorption. Both restrictive and GI bypass procedures produce significantly greater weight loss and more profound improvements in glucose tolerance than medical treatments<sup>5,6</sup>. However, the degree of improvement varies with the type of procedure used and the precise techniques utilized.

The mechanisms of the metabolic and cardiovascular improvements associated with bariatric surgery are not clearly defined. While weight loss is associated with commensurate decrements in insulin resistance, recent clinical results suggest that the GI bypass, in contrast to the restrictive procedure, normalizes insulin sensitivity even before achievement of ideal body weight<sup>7,8</sup>. A weight-independent response has been thought to initiate this amelioration in insulin resistance. Research has been carried out on a variety of large animal models of bariatric surgery, including the pig and dog<sup>9-11</sup>. These experiments support the notion that weight loss is related to reduced stomach volume and changes in the regulation of intestinal hormones. However, the mechanisms of bariatric surgery on glucose metabolism, and on hormone secretion and action remain to be elucidated. A bariatric surgery model has been developed in rats and recent findings from these studies show changes in meal patterns, satiety, food choice, glucose metabolism and energy expenditure<sup>12-14</sup>. These studies concluded that the improvement in glucose tolerance is due to increased insulin sensitivity. However, systematic studies that compare different effects of restrictive and GI bypass surgeries on weight loss and glucose metabolism remain to be performed. We have developed a repertoire of mouse bariatric surgical models to provide tools to study the physiology of bariatric surgery that can be applied to the vast number of genetic mouse models of metabolic disease. The application of bariatric surgical techniques to genetic mouse models provides a unique opportunity to test the mechanisms associated with the effects of bariatric surgery on glucose metabolism and hormone action, and elucidates the neural and immunological effects of bariatric surgery.

The development of mouse bariatric surgery models was accomplished in high fat diet-induced obese (DIO) mice. The models developed were (i) gastric banding, (ii) sleeve gastrectomy, (iii) RYGB, (iv) modified RYGB (mRYGB) and (v) BPD. A higher surgical success rate and fewer surgical complications were observed in mice with sleeve gastrectomy and mRYGB procedures, which can represent reliable restrictive and GI bypass models, respectively. Both restrictive and GI bypass procedures provide a positive effect on weight loss and glucose tolerance; however, in the long term, weight loss and improvement in fat composition, liver steatosis and glucose tolerance were more evident in GI bypass-treated mice.

## Methods

### *Mice*

C57BL/6 (H-2b) mice were purchased from Jackson Laboratory (Bar Harbor, ME). Mice expressing luciferase under the control of a NF- $\kappa$ B promoter (*NF- $\kappa$ B-luc*) on a C57BL/6 background or a mouse insulin promoter (*MIP-luc*) on a FVB background were kindly provided by Dr. Timothy Blackwell and Dr. Alvin Powers, Department of Medicine at Vanderbilt University Medical Center<sup>15, 16</sup>. Mice were housed at 23°C on a 07:00-19:00 light cycle. At 6 weeks of age the mice were placed on a 60% Kcal fat diet (Research Diets, Inc.) for 12 weeks to establish diet-induced obesity (DIO). The mice were maintained on the same high fat diet after bariatric surgery. All experiments and surgical preparations were performed according to the protocol approved by the Vanderbilt University Medical Center Institutional Animal Care and Use Committee (IACUC). The mice remained under the care of the Division of Animal Care (DAC) at Vanderbilt University in compliance with NIH guidelines and the Principles of Laboratory Animal Care, and the *Guide for the Care and Use of Laboratory Animals*.

### *Bariatric Surgical preparations:*

Animals were fasted for 4 to 6 hours prior to the surgical preparations. Surgical anesthesia was induced and maintained throughout the procedure with isoflurane (2-3% with O<sub>2</sub>). Following aseptic preparation a midline laparotomy was performed to gain exposure to the gastrointestinal tract. At the conclusion of the bariatric procedure, the midline incision was closed and the mice were recovered on a water-circulated heating pad.

*Gastric Banding:* The gastroesophageal junction was isolated and an elastic silicon rubber string (0.23mm) was placed around the gastroesophageal junction (Figure 1A). The ends of the string were tied together to form an elastic circular band with the tension of the band adjusted such that the expansion capacity of the junction is restricted as food passes into the stomach. This procedure is purely a gastric restrictive procedure. Sham procedures involved the mobilization of the esophagus and stomach, and the silicone string was placed around the gastroesophageal junction, tied and then removed.

*Sleeve Gastrectomy:* The procedure involves the excision of approximately 70 percent of the stomach. A gastric tube was fashioned along the lesser curvature with the incision line starting at the body, 1 cm distal to the gastroesophageal junction and extending to around 1 cm proximal to the pylorus along the lower great curvature. The stomach tube (1 cm in diameter) was closed using 9-0 Ethilon sutures (Figure 1B). In this fashion, gastric continuity is maintained and the greater curvature region of the stomach was eliminated. In the sham procedure, the stomach, duodenum and jejunum were mobilized and the stomach was clamped without incision.

*RYGB:* The upper gastrointestinal anatomy of the mouse does not permit the replication of the procedure that is utilized in humans. We developed a procedure that closely resembles RYGB by ligating the stomach between the glandular portion and the gastric fundus (forestomach). A portion of the jejunum, 4 cm from the Ligament of Treitz and 6 cm from the site of gastroenterostomy, was transected. The distal segment was anastomosed to the forestomach using 9-0 Ethilon in a side-to-side fashion. GI continuity is established by performing a side-to-side jejuno-jejunostomy, Figure 1C. The sham procedure involved mobilization of the forestomach and proximal and distal jejunum and ileum without any intersection.

*Modified RYGB (mRYGB):* mRYGB was developed because the forestomach of the mouse lacks sufficient muscle to push nutrients through the anastomosis in an RYGB procedure, resulting in a high mortality within a few days of surgery. mRYGB was performed in a similar fashion to the RYGB, but the upper side-to-side anastomosis of the jejunum was performed with the lower portion of the esophagus. The stomach ligation was accomplished by placing a suture to close the gastroesophageal junction distal to the anastomosis. The distances of jejunum-jejunostomy to the Ligament of Treitz and the site of gastroenterostomy are 4 cm and 6 cm, respectively, as described in Figure 1C.

*Biliopancreatic diversion (BPD):* A portion of the jejunum, 4 cm from the Ligament of Treitz and 12 cm from the site of gastroenterostomy, was transected. The distal segment was anastomosed to the greater curvature of the stomach using 10-0 Ethilon in a side-to-side fashion. Continuity of the GI tract was established by performing a side-to-side anastomosis. This procedure results in an isolation of the duodenum and uppermost segment of the jejunum from the GI tract. Unlike the human procedure, the proximal duodenum is ligated at the pyloric-duodenal junction using 6-0 silk, but not transected as shown in Figure 1E.

#### *Gastrointestinal imaging following bariatric surgery*

We evaluated GI continuity by imaging with contrast 14 days after the bariatric procedures. Mice were fasted 6hr prior to imaging (MicroCat-II, Siemens) and anesthetized with isoflurane. Contrast (Optiray 320) was administered by gavage with a volume of 0.8 ml and continuous imaging was performed.

#### *Whole body composition*

Body mass was measured using mq10 NMR analyzer (Bruker Optics Inc, Billerica, MA) following 2 hr of fasting. The NMR analyzer allows for the measurement of whole-body composition parameters, including total body fat, muscle and body fluids, in conscious rodents<sup>17</sup>. Fat, muscle and body fluids were calculated as grams of total mass.

#### *Intraperitoneal glucose tolerance tests (IPGTT)*

Mice were fasted for 4 hr prior to the IPGTT. Blood was sampled from the tail vein before and at 30, 60, 90 and 120 min after an intraperitoneal injection of 2 mg/g body weight of dextrose (20%). Blood glucose levels (mg/dL) were measured using a blood glucose meter (SureStep, Lifescan, Inc.). The area under the curve (AUC) was calculated using the trapezoidal rule<sup>18</sup>.

#### *Bioluminescence imaging (BLI)*

Bioluminescence imaging was performed under anesthesia with isoflurane. Luciferin (Roche Diagnostics, Indianapolis, IN) was injected intravenously at a dose of 50mg/kg. Mice were housed inside a light-tight box and imaged with an ICCD camera (Hamamatsu C2400-32, Hopkinton, MA). Light emission through the ventral body was detected as photon counts over a standardized area of the organs of interest using the ARGUS-50 software for image processing<sup>19-21</sup>. Islet viability was evaluated by BLI analysis using *MIP-luc* mice. NF- $\kappa$ B activation in the abdomen was measured by BLI using *NF- $\kappa$ B-luc* mice.

#### *Pathological examination*

Selected mice were sacrificed and the livers were collected for pathological examinations (H&E) following bariatric surgery. Liver histopathological features were evaluated by Brunt's grading. Significant lesions included steatosis, ballooning, and

intra-acinar and portal inflammation; and the lesion was graded as mild (1+, up to 33%), moderate (2+, 33-66%) and severe (3+, >66%)<sup>22</sup>.

### *Statistics*

Animal survival days were presented as mean survival time  $\pm$  standard deviation (MST  $\pm$  SD), and Kaplan-Meier graphs were constructed. Statistical significance was analyzed by ANOVA (Abacus Concepts, Berkeley, CA). *P*-value of  $< 0.05$  was considered significant. For *in vitro* data analysis, results are presented as mean  $\pm$  SEM, and comparisons between the values were performed using the 2-tailed Student's *t* test. The level of significance was set at a probability of  $p < 0.05$ .

## Results

### *Development of mouse bariatric surgery models*

We have developed bariatric surgery models in mice that correspond to the surgical approaches used in humans. Each surgical procedure uniquely reconfigures the gastrointestinal tract such that the physiological roles of specific segments (e.g. stomach, duodenum and jejunum) can be isolated and characterized. The success rates range from 80% to 100%. The banding procedure is usually considered a relatively simple restrictive procedure; however, it is difficult to define the banding tension (diameter) of the lower esophagus in mice. Animals died of banding restriction within one month post-surgery when the ligation was too tight (25% of mice with gastric banding). Another 25% of animals with the banding procedures failed to produce weight loss due to ineffective banding. Sleeve gastrectomy removed the greater curvature and the entire fundus (70–80% of total stomach, which includes 90% of the forestomach and 70% of the glandular stomach), and surgical success rate was 100%. In the RYGB procedure, the forestomach of the mouse lacks the elasticity and motility to develop pressures necessary to force the meal past the anastomosis, resulting in high mortality from gastric obstruction. 80% of the animals with RYGB required euthanization due to the obstruction and severe malnutrition within two weeks post-surgery. We modified the procedure by the anastomosis of the jejunum to the lower portion of the esophagus and animals with the mRYGB could eat and drink freely. Surgical success rate was 80% (Table 1). Thus sleeve gastrectomy and mRYGB represent reliable mouse gastric restrictive and GI bypass models, respectively.

Normal contrast-enhanced CT examinations in bariatric surgical procedures confirmed the specific GI reconfiguration along with GI continuity resulting from the specific bariatric surgical procedure (Fig. 2). Slight reduction of stomach volume was observed in the gastric banding procedure (Banding). The stomach volume was significantly reduced in sleeve gastrectomy (Sleeve) and RYGB procedures. The contrast passed directly into the jejunum in mRYGB procedure. No bowel obstruction and anastomotic leaks were observed.

### *Effects of bariatric surgery on total body weight loss and changes in fat mass*

The bariatric surgical procedures resulted in weight loss in all mice. The sham procedures resulted in significant weight loss; however, body weights returned to normal levels two weeks, post-surgery. There were no significant differences in body weight or glucose tolerance tests among the different sham procedures; thus, data collected from all sham surgeries was pooled and are referred to as “sham.” Both restrictive and GI bypass procedures produced weight loss ( $p < 0.05$  in all groups, compared to untreated and sham-treated DIO mice at all time points, post-surgery). The most significant weight loss was observed in mice with GI bypass procedures (mRYGB and BPD) as compared to restrictive procedures (banding and sleeve, Fig 3A).

Our results show that fat mass in DIO mice was significantly higher than that in lean mice and there was no significant difference of lean mass (Figs. 3B and C). Within one week, bariatric procedures resulted in significant reductions in fat mass with the most prominent results achieved with mRYGB and BPD, followed by sleeve gastrectomy and banding. There were no significant differences in lean mass among the groups (Fig. 3C). Although the sham surgery also impacted body mass, it was comparable to untreated DIO mice after two weeks of surgery.

Liver steatosis is a morphological pattern of DIO liver and may progress into steatohepatitis<sup>23</sup>. To test whether bariatric surgery can improve liver steatosis, we harvested livers at 4 and 8 weeks, post-surgery, for pathological examination (H&E).

According to the standards of liver steatosis grading<sup>22</sup>, the severity of all DIO livers were graded 2 to 3 (i.e. moderate to severe lesions,  $\geq 66$  percent of hepatocytes are affected). Liver steatosis was significantly improved by sleeve gastrectomy and mRYGB procedures at 4 weeks (0 - 1), compared to untreated and sham-treated DIO liver (Fig. 3D). However, mRYGB, but not sleeve gastrectomy, persistently improved liver steatosis at 8 weeks, post-bariatric surgery.

#### *Bariatric surgery improves glucose tolerance and regulates pancreatic islet viability*

Untreated DIO or sham surgery DIO mice showed glucose intolerance, compared to chow-fed mice (naïve B6) mice, as evidenced by abnormal IPGTT. Sleeve gastrectomy improved glucose tolerance in the early period (less than 4 weeks); however, there was no significant difference between untreated DIO mice and sleeve-treated DIO mice at 8 weeks, post-surgery. mRYGB and BPD procedures persistently improved glucose tolerance (Tables 2 - 5 and Fig. 4).

The effect of high fat diet and bariatric surgery on the viability of pancreatic islets was examined. FVB mice express luciferase under the control of a mouse insulin promoter (*MIP-luc*) and were utilized to visualize the viability of pancreatic islets. *MIP-luc* mice were fed a high fat diet for more than 12 weeks and subjected to BLI examinations. Enhanced luciferase activity was observed in DIO mice, compared to regular chow-fed mice of the same age (lean, Fig. 5), suggesting that DIO induces over-activation of pancreatic beta-cells. The luciferase activity was reduced in sleeve gastrectomy and mRYGB groups (*versus* untreated DIO mice,  $p < 0.05$  and  $p < 0.01$ , respectively) at 4 weeks, post-surgery. However, mRYGB procedure, but not sleeve gastrectomy, persistently improved beta cell function 8 weeks after surgery (Fig. 5).

#### *DIO induces elevated NF- $\kappa$ B activation*

It is increasingly recognized that obesity is a chronic inflammatory process characterized by macrophage infiltration of adipose tissue and liver, as well as elevated levels of cytokines involving metabolically active sites such as the liver and adipose tissue<sup>24, 25</sup>. The inflammatory response in obesity is mediated by immune cells through certain signaling pathways, including the NF- $\kappa$ B pathway<sup>25, 26</sup>. In this study, BLI was performed using NF- $\kappa$ B-driven luciferase transgenic mice. NF- $\kappa$ B activation was increased in the abdomen of DIO mice (ROI,  $10.5 \times 10^6$ ), compared to regular chow-fed mice (ROI,  $1.14 \times 10^6$ ,  $p < 0,001$ ). All bariatric surgical procedures resulted in significant activation of NF- $\kappa$ B, with the mRYGB causing the highest activation; the activation was ameliorated one week after all bariatric procedures with the highest effect noted following mRYGB (Fig. 6).

#### *Complications of bariatric surgeries*

The bariatric procedures were not associated with short-term complications (e.g. bleeding, leaking, infection and intestinal obstruction) (Table 1). The CT imaging examinations showed the patterns of bariatric surgery without leaking and obstruction of the digestive system (Fig. 2). The bariatric surgical procedures were associated with significant long-term complications, primarily malnutrition. Consistent with human data<sup>27-29</sup>, GI bypass procedures, and most prominently BPD and mRYGB, resulted in more severe anemia than noted with the restrictive procedures (gastric banding and sleeve gastrectomy). Compared to naïve lean mice ( $50.5\% \pm 3.2$ ), hematocrit levels at one month were  $22.0\% \pm 5.5$  following RYGB ( $p < 0.001$ ),  $19.5\% \pm 3.5$  following BPD ( $p < 0.01$ ),  $38.4\% \pm 3.5$  following sleeve gastrectomy ( $p = 0.414$ ), and  $33.8\% \pm 6.8$  following gastric banding mice ( $p > 0.05$ , Fig. 7). Mice with GI bypass procedures (mRYGB and BPD) experienced reduced percentages of red blood cells (RBCs, 6.4 and 3.7,  $n = 2$ ), hemoglobin (HB, 7.9 and 4.5,  $n = 2$ ) and mean cell volume (MCV, 35.5 and 29.7,  $n = 2$ ).



Additional symptoms of malnutrition included hair loss and significant weight loss 2 to 8 weeks post-surgery. 40% (mRYGB) and 80% (BPD) of the mice presented symptoms of severe malnutrition (Table 1).

## Discussion

Bariatric surgery is the most effective treatment for morbid obesity<sup>2,4</sup>. Gastric banding, RYGB and sleeve gastrectomy are widely used in the U.S. for the treatment of obesity and its comorbidities, with some centers performing BPD. A rat bariatric surgery model has been developed and used to support the notion that improvements in weight loss and diabetes are related to a variety of factors, including reduced stomach volume, changes in the regulation of intestinal hormones and increases in insulin sensitivity<sup>9, 14, 30-34</sup>. We have developed four different bariatric surgery models in DIO mice. Our results are similar in many respects to those obtained in human subjects following the commonly used bariatric procedures, namely gastric banding, sleeve gastrectomy, RYGB, mRYGB and BPD. However, in our mouse bariatric surgeries, sleeve gastrectomy and mRYGB represent reliable restrictive and GI bypass models, respectively, due to higher surgical success rates.

It is clear from our studies that both restrictive and GI bypass procedures produce positive effects on weight loss, fat composition and glucose tolerance in the short term (4 weeks); however, in the long term (8 weeks), restrictive procedures were least effective in decreasing body weight and body fat, while mRYGB and BPD were quite effective in treating obesity and insulin resistance. Therefore, the results from the present study indicate that those bariatric procedures resulting in the additional malabsorptive component (mRYGB and BPD) were the most effective. BPD resulted in the most significant losses of body weight and fat mass. It is important to note that our model of mRYGB is a modified one which requires the anastomosis of jejunum directly to the esophagus and differs from the human RYGB model where the jejunum is anastomosed to a small gastric pouch. mRYGB procedure produces weight loss as effective as standard RYGB without the high mortality. It is also important to note that while the mouse BPD model was the most effective in treating obesity, it was associated with a much higher incidence of malnutrition. Human data suggest that BPD is extremely effective in ameliorating diabetes as 90% of patients have normoglycemia and increased insulin sensitivity up to 20 years, post-surgery<sup>35</sup>.

Several studies have shown that bariatric procedures, and most significantly RYGB and BPD, ameliorate insulin resistance associated with obesity and reverse type 2 diabetes mellitus<sup>36</sup> through poorly understood mechanisms. Several of the studies have shown that the improvements associated with bariatric surgery are not solely related to weight loss. Our results offer some insight into potential mechanisms for which the models developed here can be used to gain further understanding. Abdominal adiposity significantly affects both lipid (FFAs) and glucose metabolism and, thus, is closely associated with insulin resistance<sup>37, 38</sup>. Recent findings suggest that high intrahepatic fat, but not visceral fat, is the primary marker of metabolic complications of obesity<sup>39, 40</sup>. Additionally, fatty liver or nonalcoholic fatty liver disease (NAFLD) is increasingly recognized as a condition associated with obesity that may progress to end-stage liver disease. Whether or not bariatric surgery has beneficial effects on patients with NAFLD is impossible to assess at this time due to the lack of clinical studies. The current study suggests that severe liver steatosis is observed in DIO mice and that bariatric procedures, especial mRYGB, significantly improve liver steatosis. The improvement of fatty liver in DIO mice is associated with improved glucose tolerance as evidenced by a diminished glycemic excursion in response to an IPGTT in bariatric surgery-treated DIO mice. Although both restrictive and GI bypass procedures exerted positive effects on glucose tolerance, in the long term, improved glucose tolerance and liver steatosis were observed in mRYGB-treated DIO mice, suggesting that the GI bypass procedure seems to be more effective than the restrictive procedure in treating insulin resistance.

Obese subjects maintain normoglycemia for a sustained interval before the onset of frank T2DM. This is presumably due to hyper-secretion of insulin that is sufficient to overcome insulin resistance. The availability of genetically modified mice whose islets express luciferase protein under the control of mouse insulin promoter (*MIP-luc*) provided us with the opportunity to visualize the viability of pancreatic islets. Utilizing BLI technology, we observed over-activation of pancreatic islets in DIO *MIP-luc* mice, compared to lean *MIP-luc* mice. Both restrictive and GI bypass significantly improved the over-activation of islet cells in DIO mice in 4 weeks, suggesting that the compensatory oversecretion of insulin associated with insulin resistance is rapidly reversed. However, beta cell over-activation was observed in sleeve-treated DIO mice at 8 weeks, whereas luciferase activity in mRYGB-treated DIO mice was still comparable to chow-fed lean mice. The results suggest that restrictive procedure ameliorates beta cell over-activation in the short term, and GI bypass improves beta cell function persistently, which is consistent with the improvement of glucose tolerance. Thus, GI bypass provides an approach for the reversal of insulin resistance and the regulation of beta cell activation.

Obesity is characterized by the activation of an inflammatory process in metabolically active sites such as the liver and adipose tissue<sup>24, 25, 41</sup>. Adipocyte hypertrophy induces the release of monocyte chemokines. The infiltrated macrophages, in turn, release inflammatory proteins causing further recruitment of macrophages to adipose tissue. NF- $\kappa$ B is a potent proinflammatory signal transduction molecule in innate and adaptive immune reactions<sup>42-44</sup>. NF- $\kappa$ B is activated in obesity and stimulation of I $\kappa$ B produces beneficial effects in the treatment of obesity and its comorbidities<sup>45, 46</sup>. While NF- $\kappa$ B activation has been implicated in T2DM, the visualization of NF- $\kappa$ B activation in DIO mice is lacking. Our results show that NF- $\kappa$ B activation is upregulated in the abdomen of DIO mice, compared to lean mice. Surgical procedures further stimulate elevated NF- $\kappa$ B activation, which is decreased one week after bariatric surgery. This observation could be important in formulating strategies for the evaluation of NF- $\kappa$ B activation in obesity-related T2DM and bariatric surgery.

Malabsorption causes nutritional deficiencies following bariatric surgery. The deficiency includes macronutrients, such as protein deficiency, and micronutrients, such as vitamins and trace elements<sup>47</sup>. Both mRYGB and BPD produce more severe malnutrition than gastric banding and sleeve procedures, as evidenced by anemia, hair loss and severe weight loss one month after surgery. The deficiency of iron, vitamin B12 and other micronutrients, such as copper, vitamins A and E and zinc, may contribute to bariatric surgery-induced malnutrition and anemia<sup>48</sup>.

In conclusion, we have developed mouse bariatric surgery models that can be utilized to address the effects of bariatric surgery on the treatment of obesity and T2DM. Sleeve gastrectomy and mRYGB represent reliable restrictive and GI bypass procedures, respectively, in mice. Both procedures produce positive effects on obesity and insulin resistance in the short term; but mRYGB improves metabolism in the long term. These procedures can provide significant information about the mechanisms associated with the effects of surgical intervention on obesity and its comorbidities.

## Acknowledgements

We thank Dr. Kelli Boyd, associate professor of Pathology, Vanderbilt University Medical Center, for assistance on the analysis of animal malnutrition, Dr. Todd Peterson, assistant professor, and Dr. Mohammed Tantawy, research fellow, Department of Imaging Science at Vanderbilt University Medical Center, for assistance on imaging analyses, and Mimi Eckhard, director, Division of Media Services, Section of Surgical Science at Vanderbilt University Medical Center, for helpful proofreading of the manuscript.

## Legends

Figure 1 *Mouse bariatric surgery models.* Bariatric surgeries include: A. gastric banding (Banding); sleeve gastrectomy (Sleeve); C. Roux-en Y gastric bypass (RYGB); D. modified RYGB (mRYGB); and E. biliopancreatic diversion (BPD). Surgical procedures were described in the Methods.

Figure 2. *Imaging of bariatric surgery.* After 7 to 10 days of bariatric surgery, imaging was performed using MicroCat-II. The contrast (Optiray 320, 0.8ml) was administered into the mouse by gavage. Continuous photos were taken every 4 seconds, for a total of 16 photos per mouse. Each figure represents one of 16 photos.

Figure 3. *Body weight and composition.* A. Weight loss and gain. DIO mice were weighed after bariatric and sham surgeries (n = 5 in each group except BPD\* that only one mouse was alive at 8 weeks). All mice lost weight in a few days after surgeries; however, mice with sham surgeries gained weight after one week of surgery, and mice with bariatric surgeries maintained their weight loss for more than one month. B. Body composition was measured by a NMR analyzer, as described in the Methods. Fat composition was expressed as grams per body weight (n = 4 in each group except BPD\* that only one mouse was alive at 8 weeks). C. Lean mass was also measured by a NMR analyzer (N = 4 in each group except BPD\* that only one mouse was alive at 8 weeks). D. Bariatric surgery improves hepatic steatosis (H&E, x 100, n = 3 in each group). (A), naïve lean mouse; (B), naïve DIO mouse; (C), DIO mouse with sham surgery at 4 weeks; (D), DIO mouse with sham surgery at 8 weeks; (E), DIO mouse with mRYGB at 4 weeks; (F), DIO mouse with mRYGB at 8 weeks; (G), DIO mouse with sleeve gastrectomy at 4 weeks; and (H), DIO mouse with sleeve gastrectomy at 8 weeks.

Figure 4. *Glucose tolerance tests* (also see Tables 2 – 5). DIO mice underwent intraperitoneal glucose tolerance tests (IPGTT) at 1 w, 2w, 4w and 8 w post-surgery (n = 3 - 6 in each group except BPD, in which only one mouse survived at 8 weeks). These mice were administered a 20 percent glucose solution (2g/kg) followed by tests of blood glucose with a glucose meter at 30, 60, 90, and 120 min after injection. The trapezoidal rule was used to analyze the area under the curve (AUC) for glucose (mg/dL x 120 min). At 1 week post-surgery, DIO versus Sham,  $p = 0.0517$ ; versus Banding,  $p = 0.0434$ ; versus Sleeve,  $p = 0.0257$ ; versus mRYGB,  $p = 0.0196$  and versus BPD,  $p = 0.0206$ . At 2<sup>nd</sup> week post-surgery, DIO versus Sleeve,  $p = 0.001$ ; versus mRYGB,  $p = 0.0026$  and versus BPD,  $p = 0.0004$ . At 4<sup>th</sup> week post-surgery, DIO versus Sleeve DIO,  $p = 0.0451$ ; versus mRYGB,  $p = 0.0016$ , versus BPD,  $p = 0.0067$  and versus other groups,  $p \geq 0.05$ . At 8<sup>th</sup> week, DIO versus mRYGB,  $p = 0.0006$ , versus other groups,  $p \geq 0.05$ .

Figure 5. *Bioluminescence (BLI) for islet viability.* DIO was induced in mice expressing luciferase under the control of an insulin promoter (*MIP-luc*), and BLI was performed after bariatric surgeries, compared to untreated DIO mice (DIO) and lean

mice (Lean). Luciferase was expressed as the regions of interest (ROI). The figures represent one of four BLI examinations.

Figure 6. *Bioluminescence (BLI) for NF- $\kappa$ B activation.* DIO was induced in mice expressing luciferase under the control of an NF- $\kappa$ B promoter (*NF- $\kappa$ B-luc*), and BLI was performed after bariatric surgeries, compared to untreated DIO mice (DIO) and lean mice (Lean). Luciferase was expressed as the regions of interest (ROI). The figures represent one of three BLI examinations.

Figure 7. *Hematocrit (HCT) levels in bariatric surgery-treated mice.* HCT was performed in DIO mice with different bariatric surgeries one month after bariatric surgery, compared to sham surgery (Sham), untreated-DIO (DIO) and untreated-lean mice (Lean, n = 3 - 4 in each group). \*:  $p < 0.05$ ; \*\*  $p < 0.01$ .

## REFERENCES

1. Frchetti KJ, Goldfine AB. Bariatric surgery for diabetes management. *Curr Opin Endocrinol Diabetes Obes* 2009; 16(2):119-24.
2. Goldfine AB, Shoelson SE, Aguirre V. Expansion and contraction: treating diabetes with bariatric surgery. *Nat Med* 2009; 15(6):616-7.
3. Kahn SE, Hull RL, Utzschneider KM. Mechanisms linking obesity to insulin resistance and type 2 diabetes. *Nature* 2006; 444(7121):840-6.
4. Saber AA, Elgamal MH, McLeod MK. Bariatric surgery: the past, present, and future. *Obes Surg* 2008; 18(1):121-8.
5. Cunneen SA. Review of meta-analytic comparisons of bariatric surgery with a focus on laparoscopic adjustable gastric banding. *Surg Obes Relat Dis* 2008; 4(3 Suppl):S47-55.
6. Phillips E, Ponce J, Cunneen SA, et al. Safety and effectiveness of Realize adjustable gastric band: 3-year prospective study in the United States. *Surg Obes Relat Dis* 2009; 5(5):588-97.
7. Ferrannini E, Camastra S, Gastaldelli A, et al. beta-cell function in obesity: effects of weight loss. *Diabetes* 2004; 53 Suppl 3:S26-33.
8. Guidone C, Manco M, Valera-Mora E, et al. Mechanisms of recovery from type 2 diabetes after malabsorptive bariatric surgery. *Diabetes* 2006; 55(7):2025-31.
9. Gentileschi P, Gagner M, Milone L, et al. Histologic studies of the bypassed stomach after Roux-en-Y gastric bypass in a porcine model. *Obes Surg* 2006; 16(7):886-90.
10. Davis KG, Wertin TM, Schriver JP. The use of simvastatin for the prevention of gallstones in the lithogenic prairie dog model. *Obes Surg* 2003; 13(6):865-8.
11. Sanchez-Margallo FM, Loscertales B, Diaz-Guemes I, Uson J. Technical feasibility of laparoscopic Finney pyloroplasty examined in a canine model. *Surg Endosc* 2007; 21(1):136-9.
12. Zheng H, Shin AC, Lenard NR, et al. Meal patterns, satiety, and food choice in a rat model of Roux-en-Y gastric bypass surgery. *Am J Physiol Regul Integr Comp Physiol* 2009; 297(5):R1273-82.
13. Stylopoulos N, Hoppin AG, Kaplan LM. Roux-en-Y gastric bypass enhances energy expenditure and extends lifespan in diet-induced obese rats. *Obesity (Silver Spring)* 2009; 17(10):1839-47.
14. Stearns AT, Balakrishnan A, Tavakkolizadeh A. Impact of Roux-en-Y gastric bypass surgery on rat intestinal glucose transport. *Am J Physiol Gastrointest Liver Physiol* 2009.
15. Blackwell TS, Yull FE, Chen CL, et al. Multiorgan nuclear factor kappa B activation in a transgenic mouse model of systemic inflammation. *Am J Respir Crit Care Med* 2000; 162(3 Pt 1):1095-101.
16. Fowler M, Virostko J, Chen Z, et al. Assessment of pancreatic islet mass after islet transplantation using in vivo bioluminescence imaging. *Transplantation* 2005; 79(7):768-76.
17. Shearer J, Duggan G, Weljie A, et al. Metabolomic profiling of dietary-induced insulin resistance in the high fat-fed C57BL/6J mouse. *Diabetes Obes Metab* 2008; 10(10):950-8.
18. Andrikopoulos S, Blair AR, Deluca N, et al. Evaluating the glucose tolerance test in mice. *Am J Physiol Endocrinol Metab* 2008; 295(6):E1323-32.
19. Everhart MB, Han W, Sherrill TP, et al. Duration and intensity of NF-kappaB activity determine the severity of endotoxin-induced acute lung injury. *J Immunol* 2006; 176(8):4995-5005.
20. Sadikot RT, Blackwell TS. Bioluminescence imaging. *Proc Am Thorac Soc* 2005; 2(6):537-40, 511-2.

21. Tanaka M, Swijnenburg RJ, Gunawan F, et al. In vivo visualization of cardiac allograft rejection and trafficking passenger leukocytes using bioluminescence imaging. *Circulation* 2005; 112(9 Suppl):1105-10.
22. Brunt EM, Janney CG, Di Bisceglie AM, et al. Nonalcoholic steatohepatitis: a proposal for grading and staging the histological lesions. *Am J Gastroenterol* 1999; 94(9):2467-74.
23. Brunt EM, Kleiner DE, Wilson LA, et al. Portal chronic inflammation in nonalcoholic fatty liver disease (NAFLD): a histologic marker of advanced NAFLD-Clinicopathologic correlations from the nonalcoholic steatohepatitis clinical research network. *Hepatology* 2009; 49(3):809-20.
24. Lumeng CN, Maillard I, Saltiel AR. T-ing up inflammation in fat. *Nat Med* 2009; 15(8):846-7.
25. Chiang SH, Bazuine M, Lumeng CN, et al. The protein kinase IKKepsilon regulates energy balance in obese mice. *Cell* 2009; 138(5):961-75.
26. Yeop Han C, Kargi AY, Omer M, et al. Differential effect of saturated and unsaturated free fatty acids on the generation of monocyte adhesion and chemotactic factors by adipocytes: dissociation of adipocyte hypertrophy from inflammation. *Diabetes*; 59(2):386-96.
27. Xanthakos SA. Nutritional deficiencies in obesity and after bariatric surgery. *Pediatr Clin North Am* 2009; 56(5):1105-21.
28. Xanthakos SA, Inge TH. Nutritional consequences of bariatric surgery. *Curr Opin Clin Nutr Metab Care* 2006; 9(4):489-96.
29. Toh SY, Zarshenas N, Jorgensen J. Prevalence of nutrient deficiencies in bariatric patients. *Nutrition* 2009; 25(11-12):1150-6.
30. Aguirre V, Stylopoulos N, Grinbaum R, Kaplan LM. An endoluminal sleeve induces substantial weight loss and normalizes glucose homeostasis in rats with diet-induced obesity. *Obesity (Silver Spring)* 2008; 16(12):2585-92.
31. Lopez PP, Nicholson SE, Burkhardt GE, et al. Development of a Sleeve Gastrectomy Weight Loss Model in Obese Zucker Rats. *J Surg Res* 2008.
32. Mistry SB, Omana JJ, Kini S. Rat models for bariatric surgery and surgery for type 2 diabetes mellitus. *Obes Surg* 2009; 19(5):655-60.
33. Kampe J, Brown WA, Stefanidis A, et al. A rodent model of adjustable gastric band surgery-implications for the understanding of underlying mechanisms. *Obes Surg* 2009; 19(5):625-31.
34. Thaler JP, Cummings DE. Minireview: Hormonal and metabolic mechanisms of diabetes remission after gastrointestinal surgery. *Endocrinology* 2009; 150(6):2518-25.
35. Scopinaro N, Marinari GM, Camerini GB, et al. Specific effects of biliopancreatic diversion on the major components of metabolic syndrome: a long-term follow-up study. *Diabetes Care* 2005; 28(10):2406-11.
36. Kashyap S, Belfort R, Gastaldelli A, et al. A sustained increase in plasma free fatty acids impairs insulin secretion in nondiabetic subjects genetically predisposed to develop type 2 diabetes. *Diabetes* 2003; 52(10):2461-74.
37. Rijkkelijkhuizen JM, Doesburg T, Girman CJ, et al. Hepatic fat is not associated with beta-cell function or postprandial free fatty acid response. *Metabolism* 2009; 58(2):196-203.
38. Gastaldelli A, Cusi K, Pettiti M, et al. Relationship between hepatic/visceral fat and hepatic insulin resistance in nondiabetic and type 2 diabetic subjects. *Gastroenterology* 2007; 133(2):496-506.
39. Fabbrini E, Magkos F, Mohammed BS, et al. Intrahepatic fat, not visceral fat, is linked with metabolic complications of obesity. *Proc Natl Acad Sci U S A* 2009; 106(36):15430-5.

40. Fabbrini E, Tamboli RA, Magkos F, et al. Surgical removal of omental fat does not improve insulin sensitivity and cardiovascular risk factors in obese adults. *Gastroenterology*.
41. Shoelson SE, Lee J, Goldfine AB. Inflammation and insulin resistance. *J Clin Invest* 2006; 116(7):1793-801.
42. Hazeki K, Masuda N, Funami K, et al. Toll-like receptor-mediated tyrosine phosphorylation of paxillin via MyD88-dependent and -independent pathways. *Eur J Immunol* 2003; 33(3):740-7.
43. Yamamoto M, Sato S, Hemmi H, et al. Role of adaptor TRIF in the MyD88-independent toll-like receptor signaling pathway. *Science* 2003; 301(5633):640-3.
44. Takeda K, Akira S. TLR signaling pathways. *Semin Immunol* 2004; 16(1):3-9.
45. Aljada A, Garg R, Ghanim H, et al. Nuclear factor-kappaB suppressive and inhibitor-kappaB stimulatory effects of troglitazone in obese patients with type 2 diabetes: evidence of an antiinflammatory action? *J Clin Endocrinol Metab* 2001; 86(7):3250-6.
46. Ghanim H, Garg R, Aljada A, et al. Suppression of nuclear factor-kappaB and stimulation of inhibitor kappaB by troglitazone: evidence for an anti-inflammatory effect and a potential antiatherosclerotic effect in the obese. *J Clin Endocrinol Metab* 2001; 86(3):1306-12.
47. Koch TR, Finelli FC. Postoperative metabolic and nutritional complications of bariatric surgery. *Gastroenterol Clin North Am*; 39(1):109-24.
48. von Drygalski A, Andris DA. Anemia after bariatric surgery: more than just iron deficiency. *Nutr Clin Pract* 2009; 24(2):217-26.



Table 1. Mouse bariatric surgery model

| Model   | Number | Success %* | Mortality%**      |
|---------|--------|------------|-------------------|
| Banding | 12     | 100        | 25 (restriction)  |
| Sleeve  | 14     | 100        | 0                 |
| RYGB    | 8      | 90         | 100 (obstruction) |
| mRYGB   | 12     | 80         | 40 (malnutrition) |
| BPD     | 10     | 90         | 80 (malnutrition) |
| Sham*** | 23     | 100        | 0                 |

\*: Success, surgical success rate.

\*\*: Mortality, mice due to the restriction of banding, obstruction in the site of anastomosis (RYGB) and severe malnutrition (RYGB, mRYGB and BPD) two months post-surgery were euthanized.

\*\*\*: Sham surgeries include all sham surgeries related to individual bariatric surgery.

Table 2. IPGTT in mice with bariatric surgeries at 1 week post-surgery (mg/dL)

| Model*        | 0min   | 30min   | 60min  | 90min   | 120min   |
|---------------|--------|---------|--------|---------|----------|
| Lean (n=4)    | 148±13 | 314±49  | 181±9  | 156±4   | 145±1    |
| DIO (n=6)     | 182±14 | 464±36  | 401±38 | 354±22  | 301±13** |
| Sham (n=3)    | 141±30 | 376±67  | 278±21 | 211±39  | 174±42   |
| Banding (n=3) | 126±12 | 298±102 | 210±82 | 190±127 | 183±76   |
| Sleeve (n=3)  | 126±30 | 412±62  | 203±57 | 160±35  | 139±30   |
| mRYGB (n=3)   | 105±18 | 373±88  | 203±66 | 163±55  | 119±25   |
| BPD (n=3)     | 117±2  | 368±113 | 205±78 | 142±31  | 110±16   |

\* Model: Lean, chow-fed lean C57BL/6 mice; DIO, high fat diet-induced obesity; Sham, DIO mice with sham surgery; Banding, DIO mice with gastric banding; Sleeve, DIO mice with sleeve gastrectomy; mRYGB, DIO mice with mRYGB; and BPD, DIO mice with BPD.

\*\* : DIO *versus* Lean at 120 min,  $p < 0.0001$ , *versus* Sham,  $p = 0.0074$ , *versus* Banding,  $p = 0.0624$ , *versus* Sleeve,  $p = 0.0007$ , *versus* mRYGB,  $p = 0.0002$  and *versus* BPD,  $p < 0.0001$ .

Table 3. IPGTT in mice with bariatric surgeries at 2 weeks post-surgery (mg/dL)

| Model*        | 0min   | 30min  | 60min   | 90min   | 120min   |
|---------------|--------|--------|---------|---------|----------|
| Lean (n=4)    | 120±11 | 308±36 | 176±11  | 155±11  | 147±10   |
| DIO (n=5)     | 157±13 | 490±36 | 419±40  | 341±11  | 319±24** |
| Sham (n=3)    | 142±27 | 402±81 | 368±73  | 271±68  | 225±66   |
| Banding (n=3) | 72±6   | 381±68 | 384±108 | 396±102 | 358±90   |
| Sleeve (n=3)  | 130±25 | 257±76 | 182±9   | 153±27  | 132±32   |
| mRYGB (n=3)   | 106±25 | 297±76 | 214±32  | 134±3   | 110±11   |
| BPD (n=3)     | 91±7   | 178±32 | 139±18  | 111±18  | 98±14    |

\* Model: Lean, chow-fed lean C57BL/6 mice; DIO, high fat diet-induced obesity; Sham, DIO mice with sham surgery; Banding, DIO mice with gastric banding; Sleeve, DIO mice with sleeve gastrectomy; mRYGB, DIO mice with mRYGB; and BPD, DIO mice with BPD (n = 3 - 4 mice in each group).

\*\* : DIO *versus* Lean at 120 min,  $p = 0.0007$ , *versus* Sham,  $p = 0.1592$ , *versus* Banding,  $p = 0.6191$ , *versus* Sleeve,  $p = 0.0038$ , *versus* mRYGB,  $p = 0.0009$  and *versus* BPD,  $p = 0.0007$ .

Table 4. IPGTT in mice with bariatric surgeries at 4 weeks post-surgery (mg/dL)

| Model*        | 0min   | 30min   | 60min   | 90min   | 120min  |
|---------------|--------|---------|---------|---------|---------|
| Lean (n=3)    | 155±7  | 286±43  | 187±12  | 162±17  | 149±4   |
| DIO (n=5)     | 158±13 | 498±40  | 431±39  | 376±22  | 319±9** |
| Sham (n=3)    | 175±12 | 426±39  | 317±68  | 268±64  | 196±38  |
| Banding (n=3) | 142±19 | 431±105 | 391±124 | 353±118 | 172±88  |
| Sleeve (n=3)  | 174±9  | 445±60  | 267±49  | 197±31  | 167±25  |
| mRYGB (n=3)   | 103±16 | 314±27  | 141±26  | 132±27  | 108±17  |
| BPD (n=3)     | 128±11 | 438±39  | 219±63  | 138±16  | 121±16  |

\* Model: Lean, chow-fed lean C57BL/6 mice; DIO, high fat diet-induced obesity; Sham, DIO mice with sham surgery; Banding, DIO mice with gastric banding; Sleeve, DIO mice with sleeve gastrectomy; mRYGB, DIO mice with mRYGB; and BPD, DIO mice with BPD (N = 3 - 4 mice in each group).

\*\* : DIO *versus* Lean at 120 min,  $p < 0.0001$ , *versus* Sham,  $p = 0.099$ , *versus* Banding,  $p = 0.6302$ , *versus* Sleeve,  $p = 0.0005$ , *versus* mRYGB,  $p < 0.0001$  and *versus* BPD,  $p < 0.0001$ .

Table 5. IPGTT in mice with bariatric surgeries at 8 weeks post-surgery (mg/dL)

| Model*           | 0min   | 30min  | 60min  | 90min  | 120min   |
|------------------|--------|--------|--------|--------|----------|
| Lean (n=4)       | 152±6  | 301±33 | 195±11 | 170±9  | 151±3    |
| DIO (n=4)        | 176±10 | 479±24 | 366±17 | 274±22 | 238±29** |
| Sham (n=3)       | 155±17 | 442±33 | 338±58 | 327±82 | 274±88   |
| Banding (n=3)    | 157±5  | 540±20 | 486±8  | 422±26 | 352±38   |
| Sleeve (n=3)     | 201±54 | 381±60 | 444±50 | 405±53 | 332±62   |
| mRYGB (n=3)      | 113±7  | 312±24 | 184±19 | 135±2  | 125±2    |
| BPD <sup>#</sup> | 151    | 407    | 177    | 168    | 152      |

\* Model: Lean, chow-fed lean C57BL/6 mice; DIO, high fat diet-induced obesity; Sham, DIO mice with sham surgery; Banding, DIO mice with gastric banding; Sleeve, DIO mice with sleeve gastrectomy; mRYGB, DIO mice with mRYGB; and BPD, DIO mice with BPD (n = 3 - 4 mice in each group).

\*\* : DIO *versus* Lean at 120 min,  $p = 0.0036$ , *versus* Sham,  $p = 0.3261$ , *versus* Banding,  $p = 0.0607$ , *versus* Sleeve,  $p = 0.1945$ , *versus* mRYGB,  $p = 0.022$ .

<sup>#</sup> : Only one mouse was alive at 8<sup>th</sup> week post-BPD surgery.

Figure 1

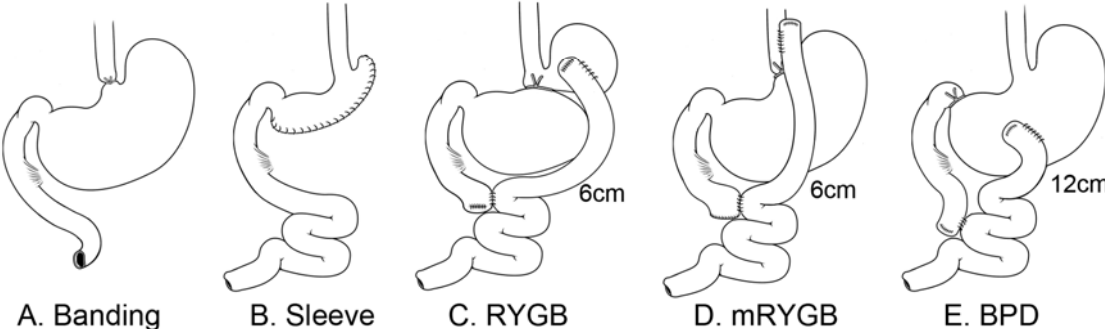


Figure 2

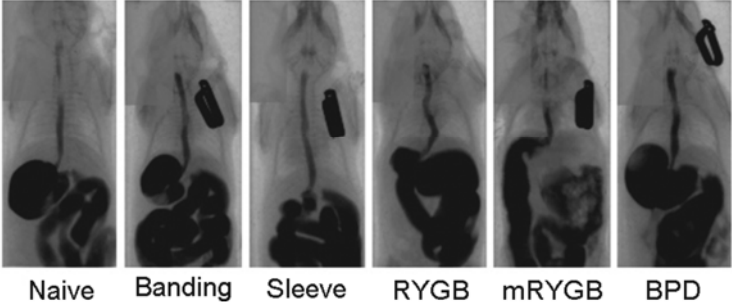


Figure 3A

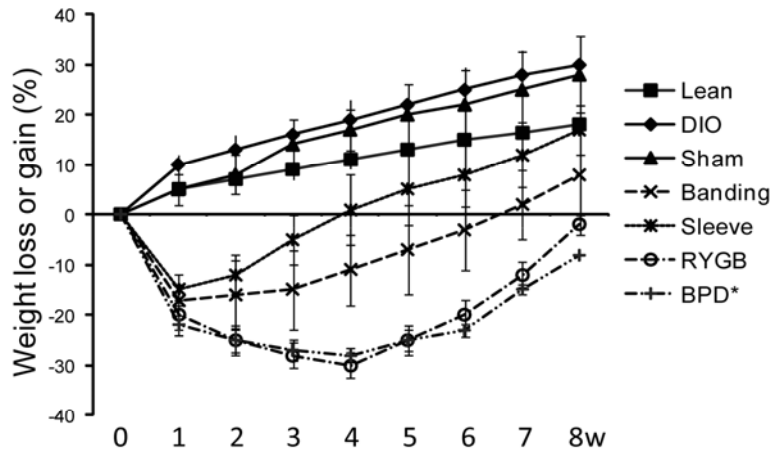


Figure 3B

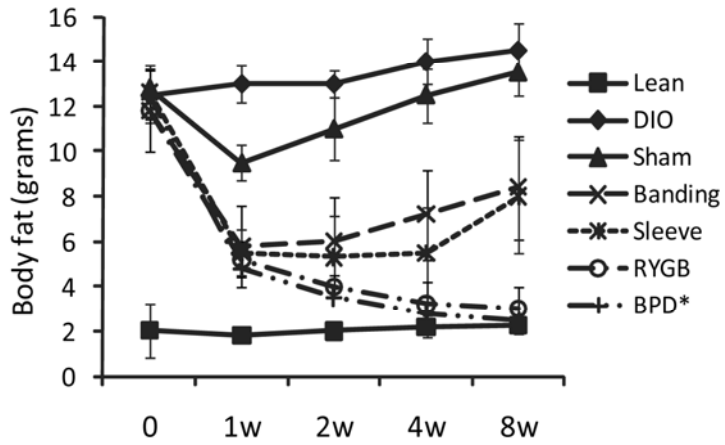


Figure 3C

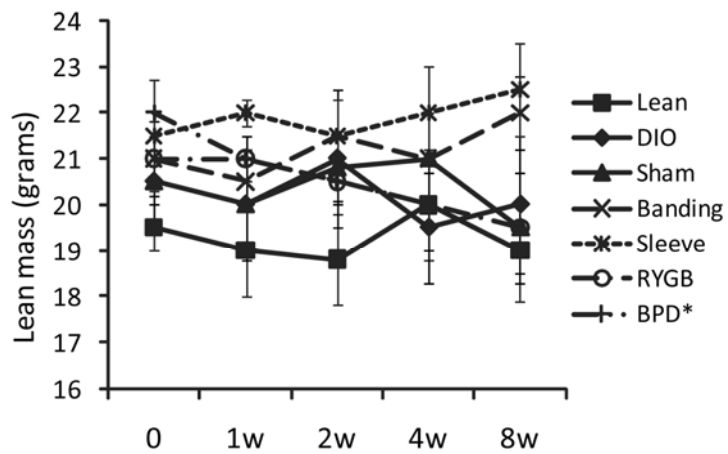


Figure 3D

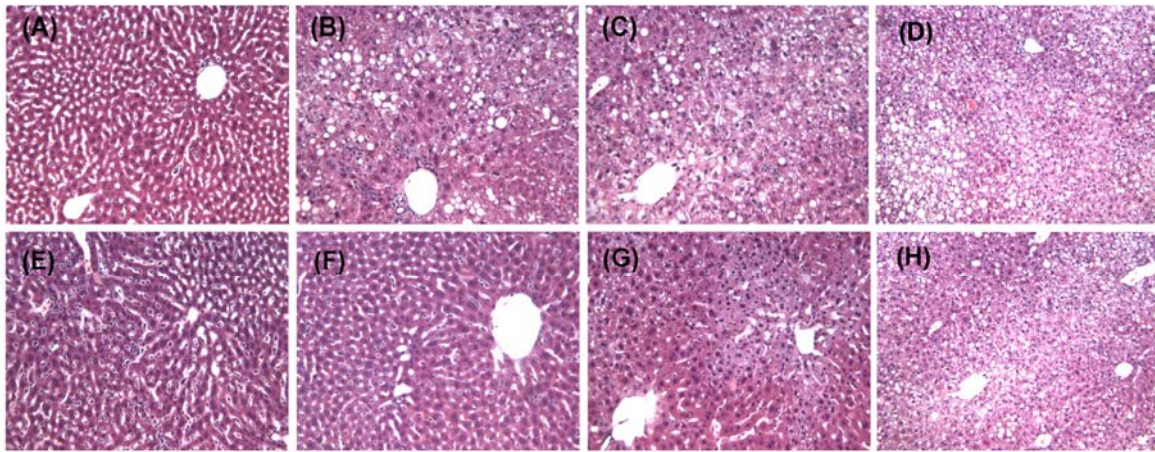


Figure 4

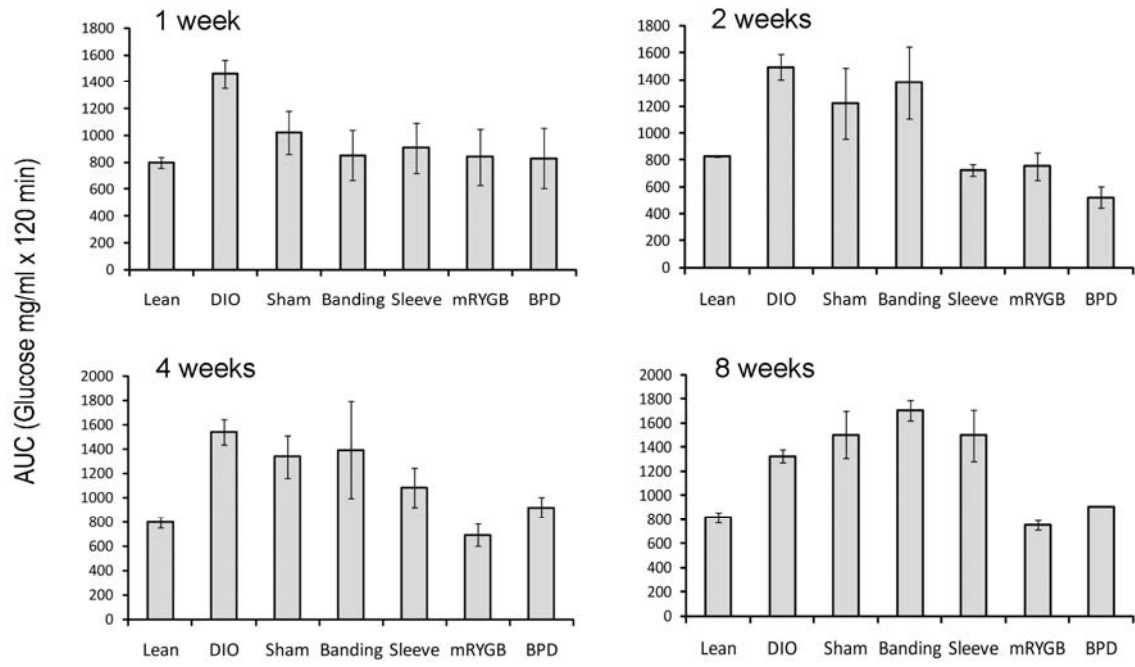


Figure 5

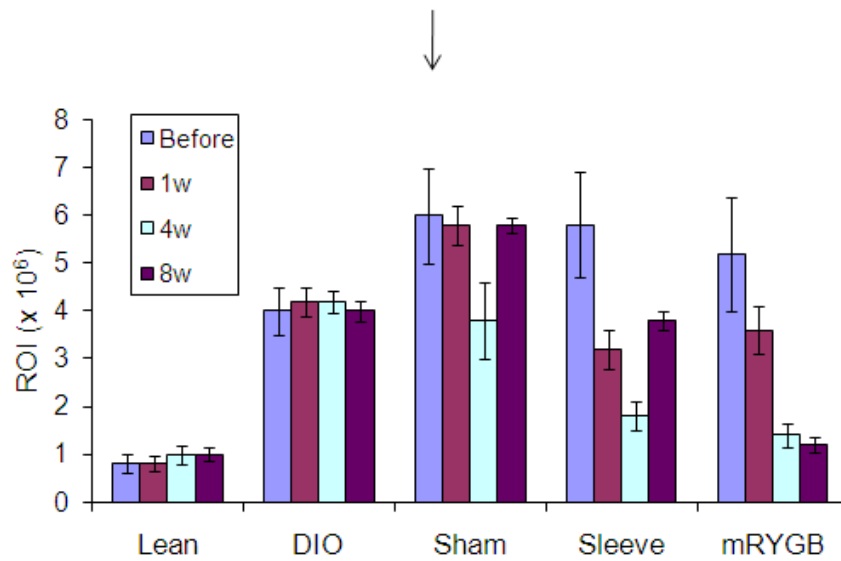
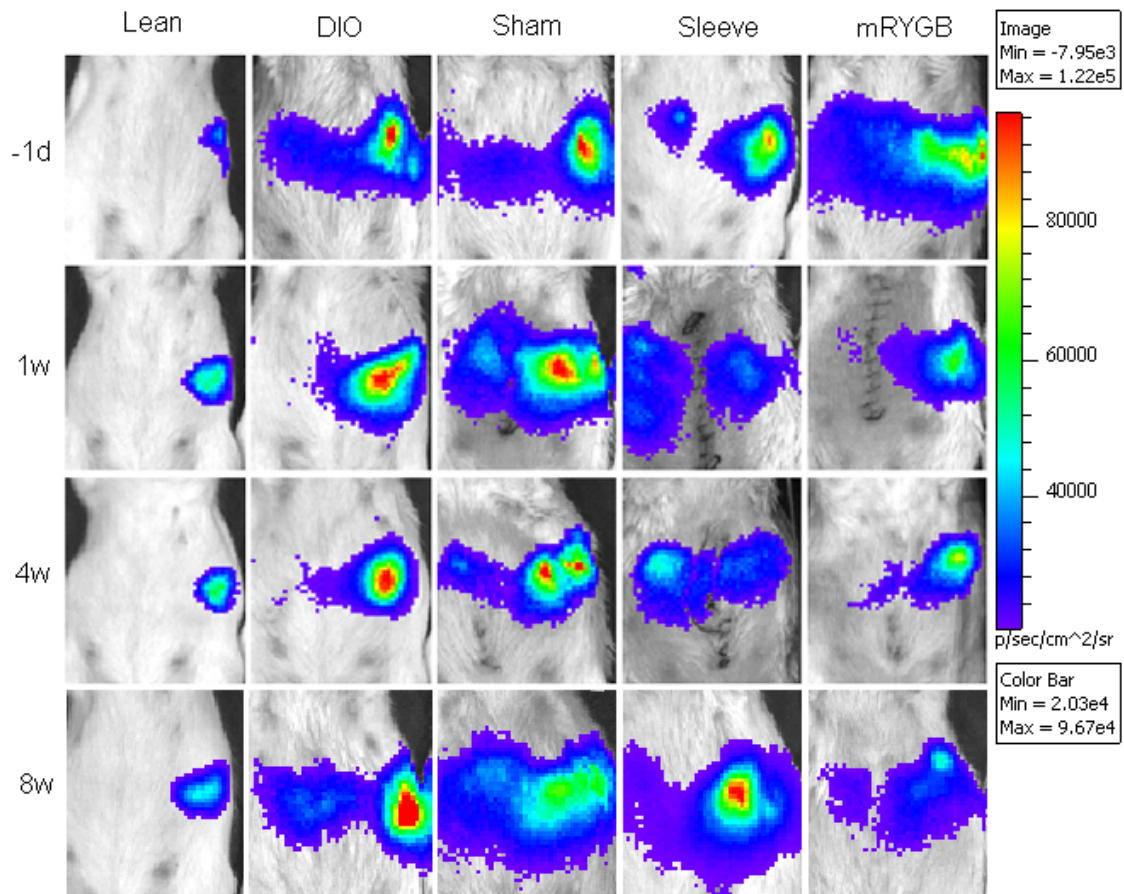




Figure 6

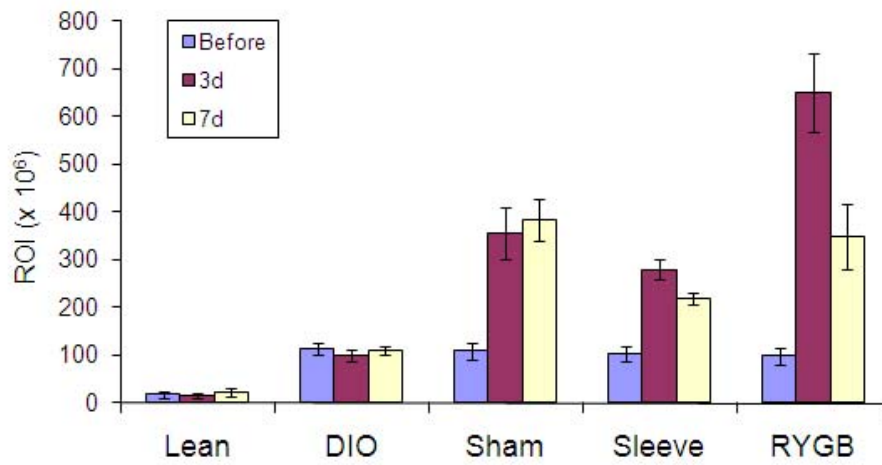
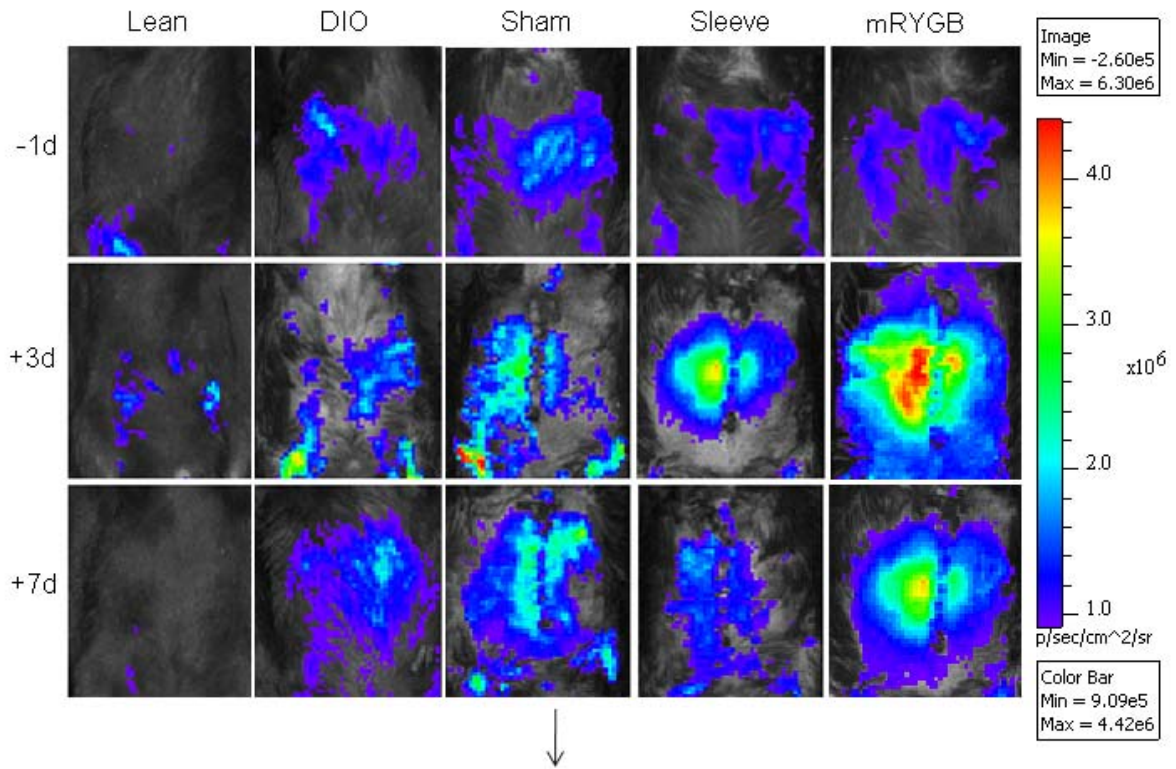


Figure 7

